An Evaluation of Inductances of a Squirrel-Cage Induction Motor Under Mixed Eccentric Conditions

Jawad Faiz, *Senior Member, IEEE*, Iman Tabatabaei Ardekanei, and Hamid A. Toliyat, *Senior Member, IEEE*

***Abstract*—This paper presents a more precise model for computation of three-phase squirrel cage induction machine inductances under different eccentric conditions. Generally, available techniques are based on the winding function theory and simplification and geometrical approximation of unsymmetrical models of the motor under mixed eccentricities. This paper determines a precise geometrical model under the mixed eccentricity conditions and evaluates the inductances. Meanwhile, the evaluated inductances are compared to those calculated using different approximate geometrical models and the best approximation is recommended for a geometrical modeling of induction motor under eccentricity conditions.**

***Index Terms*—Inductance computation, rotor and stator eccentricities, three phases induction motor, winding function approach.**

NOMENCLATURE

θ	Rotor angle (in mechanical degree)
φ	Rotor circumferential angle
$r(\varphi,\theta)$	Average radius of air-gap in nonsymmetrical conditions
$g(\varphi,\theta)$	Air-gap length in nonsymmetrical conditions
g_0	Air-gap length in symmetrical conditions
r_0	Mean radius of air-gap for symmetrical condition
l	Length of stack
R_1	Stator inner radius
R_2	Rotor radius in eccentric condition
R_r	Rotor radius in symmetrical condition
δ_s	SE coefficient
δ_d	DE coefficient
$N_i(\varphi,\theta)$	Winding function of winding i
$n_i(\varphi,\theta)$	Turn function of winding i
α_k	Pitch of slot containing winding
$\Lambda(\varphi,\theta)$	Geometrical function of induction motor
$L_{ij}(\theta)$	Mutual inductances between winding i and j

I. INTRODUCTION

INDUCTION motors have small air-gap and they are vulnerable to slight variations in the dimensions of the motors. The nonuniform air-gap distorts the air-gap flux density distribution giving rise to harmonic traveling waves of flux density. Although some approaches could significantly reduce the magnetic force wave relevant to the eccentricity that induced distortion of the air-gap flux density, the rotor remains eccentric. This imbalance performance of the motor is classified based on the type of the rotation of the rotor inside the stator bore. These are described as follows:

1) *Static Eccentricity (SE):* Static rotor eccentricity occurs when the rotor rotates about its own centerline, but this centerline does not coincide with that of the stator bore.
2) *Dynamic Eccentricity (DE):* Dynamic rotor eccentricity (DE) occurs when the rotor rotates about the centerline of the stator bore, but this centerline does not coincide with that of the rotor itself. The result is that the position of the minimum air-gap rotates with the rotor.
3) *Mixed Eccentricity (ME):* In this case, both rotor symmetrical and mechanical rotation centerlines are displaced individually in respect to the stator symmetrical centerline.

It is deduced that in the static eccentricity the functions of air-gap length and its average radius from the stator center are not constant but are independent of the rotor angular position However, in the dynamic eccentricity, in addition to the nonfixed functions, they depend on the rotor angular position. The role of these functions in the inductance calculation leads to more complicated equations and computations compared to the case in which the stator and rotor centerlines coincide. Thus, in all cases (SE, DE and ME), geometrical model of the motor is unsymmetrical and the air-gap is not uniform. Also, the air-gap mean radius is a function of the rotor circumferential angle [2]. This leads to complicated equations describing the motor. However, efficient traditional techniques such as d–q model may not be used for solving the electro-dynamic equations of the motor. Many papers have been published concerning the electric motors performance with eccentricity of the rotor and stator centerlines. In [2], [4] this has been solved from unbalance magnetic pull (UMP) computation point of view. In [5]–[7] the winding functions are used in order to estimate the inductances of the motor analytically.

Recently, a three-phase induction motor has been analyzed and simulated in the ME case using finite element (FE) technique. Generally, two approaches have been used to analyze the motor performance. The first is the magnetic field computation and the second is the direct computation of the inductances. The magnetic field computation is based on the numerical techniques such as finite elements [1]–[3], [7]. In direct computation [5], [6], [8], these inductances may be then used to predict the performance of the motor. The major difference in various analytical approaches is the type of winding functions. In [5] a modified winding function approach and in [6] step variations of winding function have been used. In recent years, the effect of linear rise of magnetomotive force or winding function considering the linear effect of MMF has been employed. Obvi-

Manuscript received November 12, 2001; revised March 2, 2002.

J. Faiz and I. Tabatabaei are with the Department of Electrical and Computer Engineering, University of Tehran, Iran.

H. A. Toliyat is with the Department of Electrical Engineering, Texas A&M University,

Digital Object Identifier 10.1109/TEC.2003.811740

ously, this approach is more precise and reliable, which takes into account more harmonics [8]. However, all available techniques simplify the geometrical model of the motor by approximating the inverse length and mean radius of the air-gap. These approximations are applied in several stages, from geometrical evaluation of these functions up to the determining the inverse of the air-gap length.

This paper determines a precise geometrical model of induction motor for general ME condition. The approximate models for SE and DE, used in different papers, are extended for a general ME condition. By comparing these models, an approximate model is recommended which is more precise than the available models without increasing the computation time. It is noted that the calculation is limitted to the geometry and several other physical problems such as local saturation and leakage flux have not been considered. Finally, evaluated inductances using this precise geometrical model are compared to the calculated inductances using other approximate models and the advantage of the proposed technique is emphasized.

II. A Precise Geometrical Model of Induction Motor for ME Condition

Different inductances of induction motor can be calculated based on the multiple coupled circuit model using winding functions, air-gap length and mean radius inverse functions. Obviously, the winding functions of the stator winding and rotor rings of the motor do not change in eccentric conditions compared to the symmetrical condition. However, the inverse functions of the air-gap length and the mean radius will change with respect to the symmetrical case. It is intended to calculate these two functions analytically, which express the geometrical model of the motor. Fig. 1 shows the geometrical model of induction motor for unsymmetrical condition.

Referring to Fig. 1, the length and the mean radius of the air-gap inverse functions are as follows:

$$\begin{cases} \frac{1}{g(\varphi,\theta)} = \frac{1}{R_1 - R_2(\varphi,\theta)} \\ r(\varphi,\theta) = \frac{R_1 + R_2(\varphi,\theta)}{2}. \end{cases} \tag{1}$$

In order to describe the geometrical model of the motor, R_2 versus the rotor circumferential angle (φ) and the rotation angle in mechanical degree (θ) must be calculated. The length of R_2 at an angle φ is obtained by intersection of the rotor circle equation and $y = x\tan\varphi$ line, while the rotor has angle θ with respect to the mechanical reference (stator axes). In order to determine

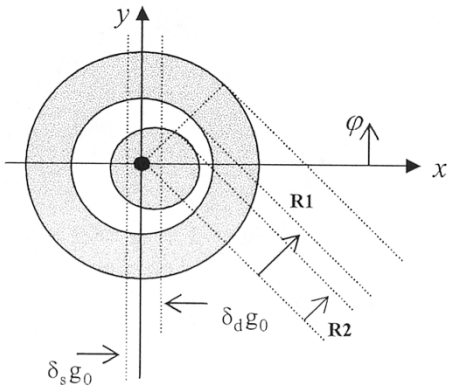

Fig. 1. Cross-section of induction motor for ME condition.

the rotor circle equation in stator frame, the following equation can be written by referring to Fig. 2.

$$(x - g_0\delta_s - g_0\delta_d\cos\theta)^2 + (y - g_0\delta_d\sin\theta)^2 = R_r^2. \tag{2}$$

Intersection of (2) and line $y = \mathrm{xtan}\varphi$ leads to the following equation: See equation (3) at the bottom of the page.Referring to (1) and (3), the following equation is obtained: See equation (4) at the bottom of the page.In order to describe the geometrical model, the geometrical characteristic is defined as follows:

$$\Lambda(\varphi,\theta) = \frac{g_0}{r_0}\frac{r(\varphi,\theta)}{g(\varphi,\theta)}. \tag{5}$$

Variation of this function for a 4 poles, 11 kW induction motor with specifications given in Appendix A [5] in different eccentricity conditions, has been shown in Fig. 3.

III. Approximate Geometrical Models for Induction Motor With Eccentricity Conditions

The first and the simplest approximation that has been used for analysis of induction motor in eccentric condition is as follows:

$$\zeta(\varphi,\theta) \approx R_r. \tag{6}$$

Thus, the geometrical characteristic of motor is simplified as

$$\Lambda_1(\varphi,\theta) = \frac{1 + \frac{\delta_s g_0}{2r_0}\cos\varphi + \frac{\delta_d g_0}{2r_0}\cos(\varphi-\theta)}{1 - \delta_s\cos\varphi - \delta_d\cos(\varphi-\theta)}. \tag{7}$$

$$\begin{aligned} R_2(\varphi,\theta) =& \delta_s g_0\cos\varphi + \delta_d g_0\cos(\varphi-\theta) + \zeta(\varphi,\theta) \\ \zeta(\varphi,\theta) =& \sqrt{R_r^2 - (\delta_s g_0\sin\varphi)^2 - (\delta_d g_0\sin(\varphi-\theta))^2 - 2\delta_s\delta_d g_0^2\cos\theta}. \end{aligned} \tag{3}$$

$$\begin{cases} g(\varphi,\theta)^{-1} = (R_1 - \delta_s g_0\cos\varphi - \delta_d g_0\cos(\varphi-\theta) - \zeta(\varphi,\theta))^{-1} \\ r(\varphi,\theta)^{-1} = 0.5\times(R_1 - \delta_s g_0\cos\varphi + \delta_d g_0\cos(\varphi-\theta) + \zeta(\varphi,\theta)). \end{cases} \tag{4}$$

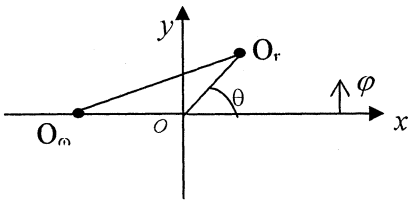

Fig. 2. Position of symmetrical axes and rotor rotation in the stator coordinates, O_r the rotor axes and $O\omega$ is the rotor rotation axes and $OO_r = g_0\delta_d$ and $OO\omega = g_0\delta$.

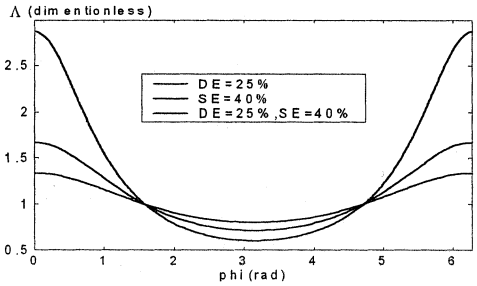

Fig. 3. Variation of geometrical characteristic of an induction motor over reference mechanical angle (φ) in different eccentricity conditions.

To calculate UMP in induction motor with static eccentricity, Dorrell [2] has shown that:

$$\frac{1}{1-\delta_s\cos\varphi} = \frac{1}{\sqrt{1-\delta_s^2}} \times\left(1+2\sum_{m=0}^{\infty}\left(\frac{1-\sqrt{1-\delta_s^2}}{\delta_s}\right)^m\cos m\varphi\right). \quad (8)$$

Although Dorrel has used an infinite series for his UMP evaluation, others employ the first two terms of the winding function. For instance, for dynamic analysis of the dynamic eccentricity, Joksimovic [5] has employed a geometrical model given by

$$\tilde{\Lambda}_2(\varphi,\theta) = \left(1+\frac{\delta_d g_0}{2r_0}\cos(\varphi-\theta)\right) \times\left(\frac{1}{\sqrt{1-\delta_d^2}}+2\frac{1-\sqrt{1-\delta_d^2}}{\sqrt{1-\delta_d^2}}\cos(\varphi-\theta)\right). \quad (9)$$

This model made approximation up to the 2nd harmonic as described below.

To analyze static and dynamic eccentricity of induction and synchronous motors, a simple geometrical characteristic of the motor has been used in [6], and by neglecting the variation of the airgap mean radius, it is considered by

$$\tilde{\Lambda}_3(\varphi,\theta) = \left(\frac{1}{\sqrt{1-\delta_d^2}}+2\frac{1-\sqrt{1-\delta_d^2}}{\sqrt{1-\delta_d^2}}\cos(\varphi-\theta)\right). \quad (10)$$

This model only takes into account the first harmonic for geometrical model of the motor as: $b_0 + b_1\cos(\varphi-\theta)$.

Non of these models describe different eccentricity conditions comprehensively and each one presents dynamic or static eccentricity. An attempt has been made to extend the model presented by Dorrell into a precise geometrical model of induction motor for a general mixed eccentricity. For this purpose, the inverse function of the air-gap length is converted as

$$\frac{1}{1-\delta_s\cos\varphi-\delta_s\cos(\varphi-\theta)} = \frac{1}{1-\delta(\theta)\cos(\varphi-\Theta(\theta))} \quad (11)$$

where:

$$\begin{cases}\delta(\theta) = \sqrt{\delta_s^2+\delta_d^2+2\delta_d\delta_s\cos\theta}\\ \Theta(\theta) = \tan^{-1}\frac{\delta_d\sin\theta}{\delta_s+\delta_d\cos\theta}\end{cases} \quad (12)$$

Based on (11) and (12), this extension is carried out. Thus, extension of the geometrical modeling techniques corresponding to Λ_2 and Λ_3 yields:

$$\Lambda_2(\varphi,\theta) = \left(1+\frac{\delta(\theta)g_0}{2r_0}\cos(\varphi-\Theta(\theta))\right) \times\left(\frac{1}{\sqrt{1-\delta(\theta)^2}}+2\frac{1-\sqrt{1-\delta(\theta)^2}}{\sqrt{1-\delta(\theta)^2}} \times\cos(\varphi-\Theta(\theta))\right) \quad (13)$$

$$\Lambda_3(\varphi,\theta) = \frac{1}{\sqrt{1-\delta(\theta)^2}}+2\frac{1-\sqrt{1-\delta(\theta)^2}}{\sqrt{1-\delta(\theta)^2}} \times\cos(\varphi-\Theta(\theta)) \quad (14)$$

where $\delta(\theta)$ and Θ are calculated according to (12). Fig. 4 compares the percentage of error for these two models in respect to the actual model and it shows that model Λ_2 is only 1 to 2% more accurate than model Λ_3, while computational time is considerably longer.

Fig. 4 indicates that the errors of 2nd and 3rd techniques in ME condition are same when 3rd technique has more computation. In the remaining part, it is shown that if the air-gap mean radius is ignored and instead one term of expansion of series (8) is included, a precise geometrical model is obtained without change of computation time. Therefore:

$$\Lambda_4(\varphi,\theta) = \frac{1}{\sqrt{1-\delta(\theta)^2}}+2\frac{1-\sqrt{1-\delta(\theta)^2}}{\sqrt{1-\delta(\theta)^2}}\cos(\varphi-\Theta(\theta)) +2\left(\frac{1-\sqrt{1-\delta(\theta)^2}}{\sqrt{1-\delta(\theta)^2}}\right)^2\cos(2\varphi-2\Theta(\theta)). \quad (15)$$

Fig. 5 compares the relative error of this model with mode Λ_2. As seen, the error of the proposed model is 2 to 3 times lower than other models.

IV. Inductances of Induction Motor for Eccentricity Conditions

Generally, MMF of the air-gap produced by current i_A of winding A at angle φ in respect to the stationary stator reference is given by

$$F_A(\varphi,\xi) = N_A(\varphi,\xi)\,i_A. \quad (16)$$

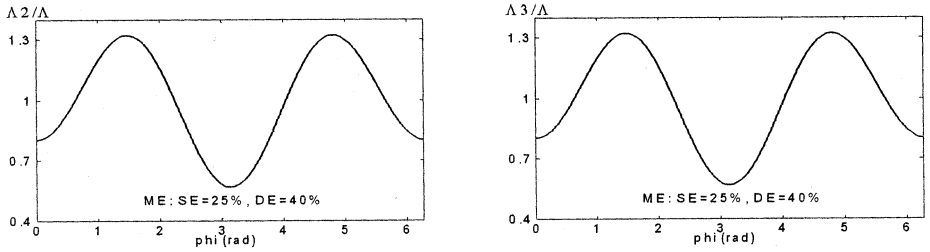

Fig. 4. Comparison of relative error of geometrical models Λ_2 and Λ_3.

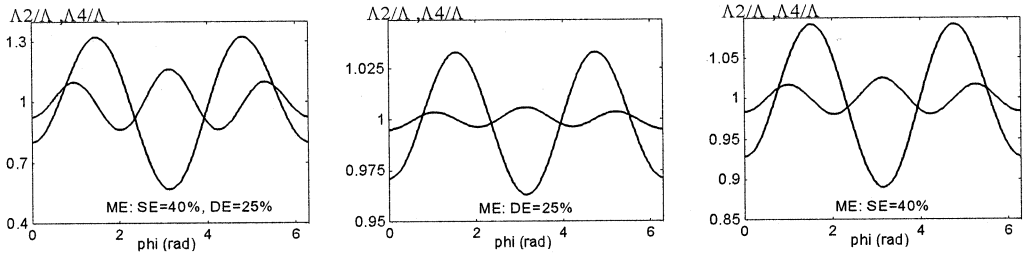

Fig. 5. Comparison of relative error of the suggested models.

Where $N_A(\varphi,\xi)$ is the winding function of winding A. Referring to Fig. 1, the differential of magnetic flux due to winding A which crosses the corresponding air-gap over angle φ is:

$$d\Psi = \frac{\mu_0 F_A(\varphi,\xi)\, r(\varphi,\xi)}{g(\varphi,\xi)} d\varphi d\xi. \tag{17}$$

Where $g(\varphi,\xi)$ is the air-gap length, and $r(\varphi,\xi)$ is the mean radius of the air-gap. The differential of flux-linkage between winding A and B is calculated as follows:

$$d\Psi_{BA} = \mu_0 \frac{r(\varphi,\xi)}{g(\varphi,\xi)} N_A(\varphi,\xi)\, n_B(\varphi,\xi)\, i_A d\varphi d\xi \tag{18}$$

where $n_B(\varphi,\xi)$ is the turns function of winding B. Taking into account the rotor mechanical angle:

$$L_{BA} = \mu_0 \int_{-l/2}^{+l/2} \int_0^{2\pi} \frac{r(\varphi,\xi)}{g(\varphi,\xi)} N_A(\varphi,\xi)\, n_B(\varphi,\xi)\, d\varphi d\xi \tag{19}$$

If the center lines of stator and rotor are in parallel and the rotor bars are assumed in parallel to the stator center line and symmetric around the center line and symmetric around the rotor cylinder, (19) will be written as:

$$L_{BA} = \mu_0 l \int_0^{2\pi} \frac{r(\varphi,\xi)}{g(\varphi,\xi)} N_A(\varphi,\xi)\, n_B(\varphi,\xi)\, d\varphi d\xi. \tag{20}$$

It is noted that generally $n_B(\varphi,\xi)$ cannot be replaced by $N_B(\varphi,\xi)$ in (20) and this assumption is valid for symmetrical and uniform air-gap. Using the geometrical characteristic of the motor leads to:

$$L_{BA} = \mu_0 l \int_0^{2\pi} \Lambda(\varphi,\xi)\, N_A(\varphi,\xi)\, n_B(\varphi,\xi)\, d\varphi d\xi. \tag{21}$$

All inductances of induction motor can be calculated from (21) using winding functions and geometrical characteristic of the motor. The winding function method is an analytical technique in the actual space in which all space harmonics of the winding MMF are taken into account. A salient feature of this technique is its capability to simulate the mechanical asymmetry and fault of stator and rotor windings. The winding function used in this work takes into account the linear variation of MMF on the slots. Figs. 6 and 7 show the turn functions of the motor.

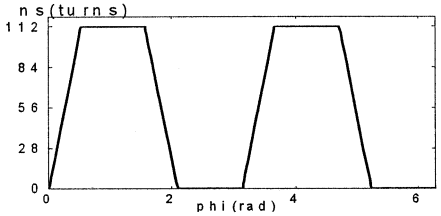

Fig. 6. Turns functions of the stator phase A.

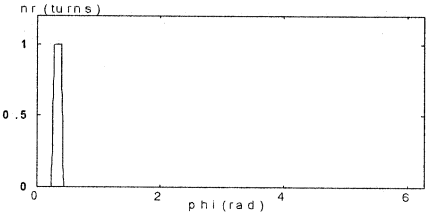

Fig. 7. Turns functions of the rotor loop 1.

V. Calculation of Inductances

In this section, inductances of the induction motor for different eccentric conditions (SE, DE and ME) are calculated. This is carried out using the precise geometrical model (λ), the approximate geometrical model of Joksimovic (λ_2), and the suggested approximate geometrical model (λ_4).

A. Self- and Mutual Inductances of Stator Phases

In symmetrical case, these inductances are independent of the rotor mechanical angle. Generally, in ME case they are function

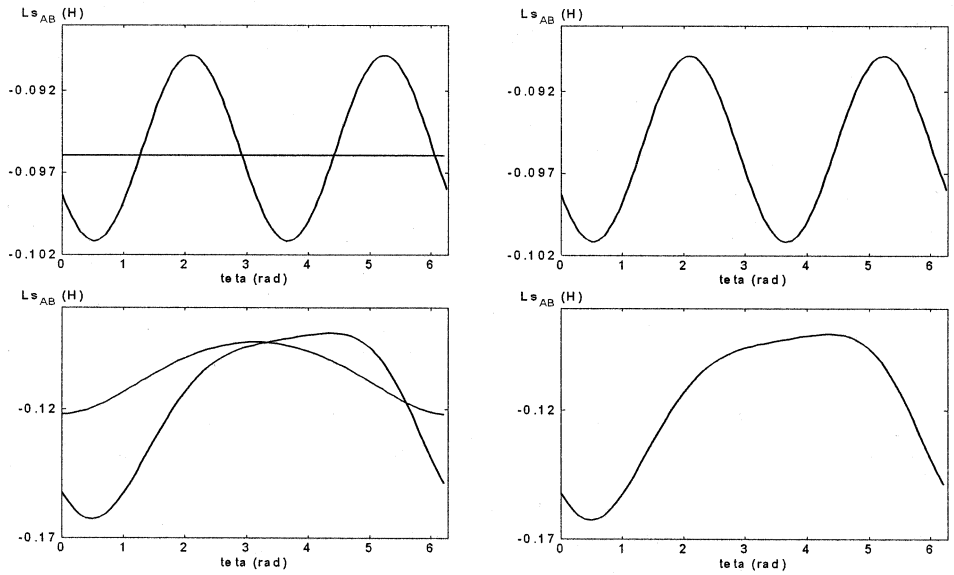

Fig. 8. Mutual inductance between phase A and B of stator Top: $\mathrm{DE} = \%25$, Bottom: ($\mathrm{DE} = 25\%$, $\mathrm{SE} = 40\%$).

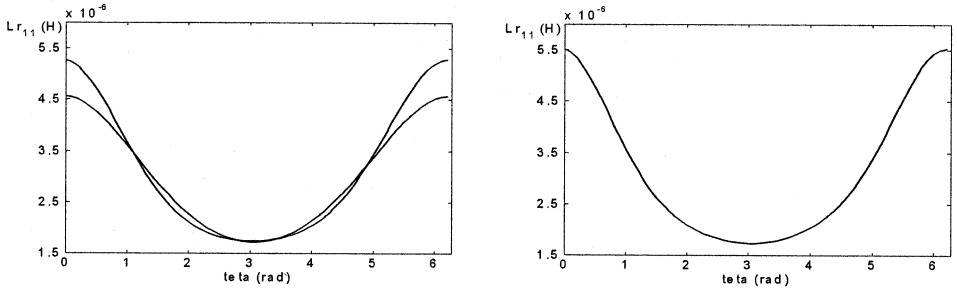

Fig. 9. Self inductance of rotor loop 1: ($\mathrm{DE} = 25\%$, $\mathrm{SE} = 40\%$).

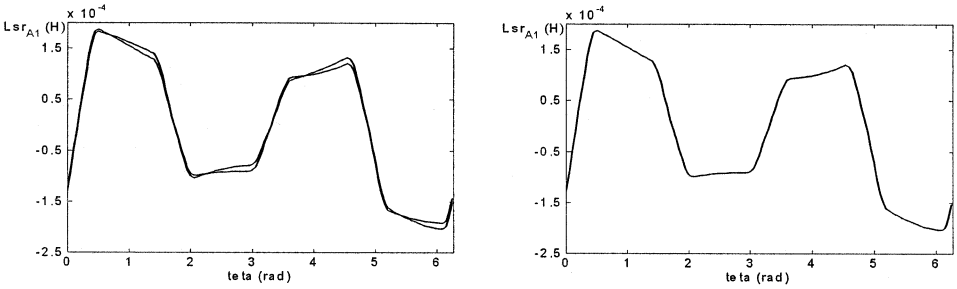

Fig. 10. Mutual inductance between the first loop of the rotor and stator phase A ($\mathrm{DE} = 25\%$, $\mathrm{SE} = 40\%$).

of θ. It can be shown that in a $2p$ pole induction motor taking into account $p+1$ harmonics and above, the angle θ appears in the stator inductances calculation. The weaker approximations of geometrical model leads to a linear rise of the inductance compared to the symmetrical case. It is noted that in SE case these inductances are independent of θ. Fig. 8 shows the mutual inductance between phase A and B of the stator. It indicates that the suggested geometrical model largely increases the accuracy of the inductance calculation. As shown in this figure, the mutual inductances of stator phase in the dynamic eccentricity obtained by the proposed and exact models, depends upon θ, but these inductances are independent of θ if the model presented in [9] is used.

B. Self- and Mutual Inductances of the Rotor Loops

It is clear that the inductance between rotor turns in DE case is independent of the rotor angle. But in SE case it is a function of angle θ. Fig. 9 presents the self-inductance of the first turn of the rotor in ME case.

C. Mutual Inductances between Rotor and Stator

Fig. 10 shows the mutual inductance between the first rotor loop of and phase a of the stator for different eccentric cases. As seen, the suggested approximate geometrical model agrees well with the results of the precise model.

Mutual inductances between the stator phases and the rotor turns are not equal to the mutual inductances between the rotor

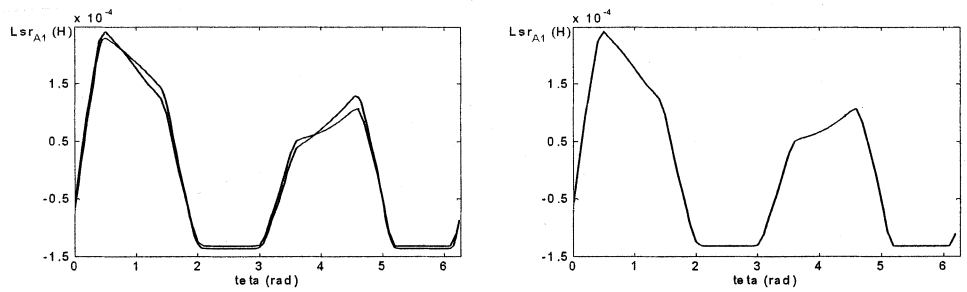

Fig. 11. Mutual inductance between stator phase A and the first loop of the rotor ($\mathrm{DE} = 25\%, \mathrm{SE} = 40\%$).

TABLE I
SPECIFICATIONS OF THE PROPOSED INDUCTION MOTOR

Output power	11 kW
L	11 cm
r	8.2 cm
Number of stator slots	48
Number of winding turns per phase group	4
Number of turns per winding	28
Number of rotor bars	40
View angle of stator bars against the stator center	$\frac{\pi}{86}$

turns and stator phases, for different eccentricities. Fig. 11 shows the mutual inductance between the stator and the fist turn of the rotor. These figures also indicate the accuracy of the proposed technique.

VI. CONCLUSIONS

Although the number of terms in the proposed geometrical model is the same as the model given in [9], the method presented in this paper is more accurate, as shown in Figs. 8–11. This leads to an improved performance prediction of induction motor. It has also been shown that by taking into account $p+1$ harmonics, the influence of angle θ apprears in the calculation of the stator inductances. This results an increase in the accuracy of calculating machine inductances. Thus, in the analysis of induction motors having large number of poles, a precise geometrical model must be used or extra terms of the expansion given by Dorrel must be considered.

APPENDIX
SPECIFICATIONS OF THE PROPOSED INDUCTION MOTOR

See Table I.

REFERENCES

[1] X. Lou *et al.*, "Multiple coupled circuit modeling in induction machines," in *Proceedings of the IEEE IAS Annual Meeting*, vol. 1, Toronto, Canada, 1993, pp. 203–210.

[2] D. G. Dorrell, W. T. Thomson, and S. Roach, "Combined effects of static and dynamic eccentricity and airgap flux waves and the application of current monitoring to detect dynamic eccentricity in 3-phase induction motors," in *IEE Conference on Electrical Machines and Drives*, 1995, pp. 151–155.

[3] M. J. DeBortoli, S. J. Salon, and C. J. Slavic, "Effect of rotor eccentricity and parallel winding on induction machine behavior: A study using finite element analysis," *IEEE Trans on Magnetics*, vol. 29, no. 2, pp. 1676–1682, March 1993.

[4] A. C. Smith and D. G. Dorrell, "Calculation and measurement of unbalanced magnetic pull in cage induction motors with eccentric rotor: Part I: Analytical model," *IEE Proceedings*, pt. B, vol. 143, no. 3, pp. 202–210, May 1996.

[5] G. M. Joksimovic, J. Penman, and N. Arthur, "Dynamic simulation of dynamic eccentricity in induction machines-winding function approach," *IEEE Trans. on Energy Conversion*, vol. 15, no. 2, pp. 143–149, June 2000.

[6] S. Nandi, H. A. Toliyat, and A. G. Parlos, "Performance analysis of a single phase induction motor under eccentric conditions," in *IEEE Industry Application Society Annual Meeting*, October 5–9, 1997, pp. 210–218.

[7] H. A. Toliyat, M. S. Arefeen, and A. G. Parlos, "A method for dynamic simulation and detection of air-gap eccentricity in induction machines," *IEEE Trans. on Industry Applications*, vol. 32, no. 4, pp. 631–636, 1996.

[8] S. Nandi, "Fault Analysis for Condition Monitoring of Induction Motors," Ph.D. Dissertation, Department of Electrical Engineering, Texas A&M Univ., College Station, TX, May 2000.

[9] G. M. Joksimovic, D. M. Durovic, and B. A. Obradovic, "Skew and linear rise of MMF across slot modeling-winding function approach," *IEEE Trans. on Energy Conversion*, vol. 14, no. 3, pp. 315–320, September 1999.

Jawad Faiz (M'90, SM'93) received the Bachelor and Master's degrees in electrical engineering from Tabriz University in Iran in 1974 and 1975 respectively graduating with First Class Honors. He received the Ph.D. degree in Electrical Engineering from the University of Newcastle upon Tyne, England in 1988. Early in his career, he served as a faculty member in Tabriz University for 10 years. After obtaining Ph.D. degree he rejoined Tabriz University where he held the position of Assistant Professor from 1988 to 1992, Associate Professor from 1992 to 1997, and has been a Professor since 1998. Since February 1999 he has been working as a Professor at the Department of Electrical and Computer Engineering, Faculty of Engineering, University of Tehran. He is the author of 115 publications in international journals and conference proceedings. Dr. Faiz is a Senior Member of Power Engineering, Industry Applications, Power Electronics, Industrial Electronics, Education and Magnetics Societies of the IEEE. He is also a member of Iran Academy of Science. His teaching and research interests are in switched reluctance and VR motors design, and design and modeling of electrical machines and drives.

Iman Tabatabaei Ardekanei obtained B.Sc. degree from Department of Electrical and Computer engineering of Tehran University in control engineering in 2000. He is currently working toward his M.Sc. degree in the same university. His research interests include induction machine modeling, induction machine analysis under fault conditions and Interior Permanent Magnet machine control.

Hamid A. Toliyat (S'87-M'91-SM'96) received the B.S, degree from Sharif University of Technology, Tehran, Iran in 1982, the M.S. degree from West Virginia University, Morgantown, WV in 1986, and the Ph.D. degree from University of Wisconsin-Madison, Madison, WI in 1991, all in electrical engineering. He is currently a professor in the Department of Electrical Engineering, Texas A&M University. He has received the Texas A&M Select Young Investigator Award in 1999, and Eugene Webb Faculty Fellow Award in 2000. He has also received the Space Act Award by NASA in 1999, and the Schlumberger Foundation Technical Award in 2000 and 2001. Dr. Toliyat is an Editor of IEEE Transactions on Energy Conversion, an Associate Editor of IEEE Transactions on Power Electronics, and a member of the Editorial Board of Electric Machines and Power Systems Journal. He is serving on several IEEE committees and subcommittees, and is a member of Sigma Xi. He is the recipient of the 1996 IEEE Power Engineering Society Prize Paper Award. His main research interests and experience include multi-phase variable speed drives for traction and propulsion applications, fault diagnosis of electric machinery, analysis and design of electrical machines, and sensorless variable speed drives.